AD-A175 398 GEOMETRIC UNIVERSALITY IN BRAIN ALLOSTERIC PROTEIN DYNAMICS: COMPLEX HYDR..(U) CALIFORNIA UNIV SAN DIEGO LA JOLLA DEPT OF PSYCHIATRY A J MANDELL ET AL. 1/1

UNCLASSIFIED 01 OCT 86 ARO-19481.13-LS DAAG29-83-K-0069 F/G 6/1 NL

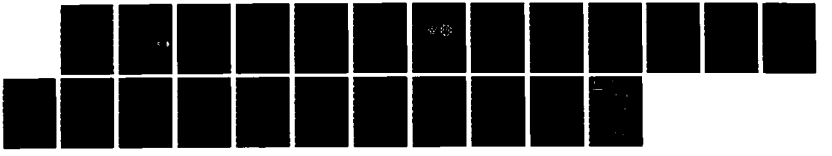

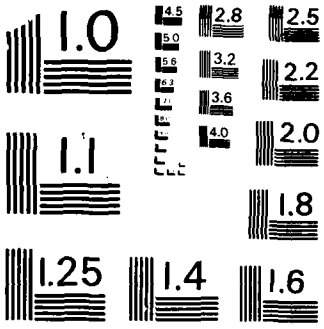

MICROCOPY RESOLUTION TEST CHART

NATIONAL BUREAU OF STANDARDS - 1963 - A

(2)

MASTER COPY - FOR REPRODUCTION PURPOSES

UNCLASSIFIED
SECURITY CLASSIFICATION OF THIS PAGE (When Data Entered)

REPORT DOCUMENTATION PAGE		READ INSTRUCTIONS BEFORE COMPLETING FORM
1. REPORT NUMBER: ARO 19481.13-LS	2. GOVT ACCESSION NO.: N/A	3. RECIPIENT'S CATALOG NUMBER: N/A
4. TITLE (and Subtitle): GEOMETRIC UNIVERSALITY IN BRAIN ALLOSTERIC PROTEIN DYNAMICS: COMPLEX HYDROPHOBIC TRANSFORMATION PREDICTS MUTUAL RECOGNITION BY POLYPEPTIDES AND PROTEINS		5. TYPE OF REPORT & PERIOD COVERED 6. PERFORMING ORG. REPORT NUMBER
7. AUTHOR(s): Arnold J. Mandell, Patrick V. Russo, and Barbara W. Blomgren		8. CONTRACT OR GRANT NUMBER(s): DAAG29-83-K-0069
PERFORMING ORGANIZATION NAME AND ADDRESS: Arnold J. Mandell, M.D. (M-003), Dept. of Psychiatry (Biol. Dyn. & Theor. Med.), Sch. of Medicine, Univ. of California, San Diego, La Jolla, CA 92093		10. PROGRAM ELEMENT, PROJECT, TASK AREA & WORK UNIT NUMBERS
CONTROLLING OFFICE NAME AND ADDRESS: U. S. Army Research Office, Post Office Box 12211, Research Triangle Park, NC 27709		12. REPORT DATE: 10/1/86 13. NUMBER OF PAGES
MONITORING AGENCY NAME & ADDRESS (if different from Controlling Office)		15. SECURITY CLASS. (of this report): Unclassified 15a. DECLASSIFICATION/DOWNGRADING SCHEDULE

DISTRIBUTION STATEMENT (of this Report)

Approved for public release; distribution unlimited.

DTIC ELECTE DEC 3 0 1986 D

17. DISTRIBUTION STATEMENT (of the abstract entered in Block 20, if different from Report)

NA

18. SUPPLEMENTARY NOTES

The view, opinions, and/or findings contained in this report are those of the author(s) and should not be construed as an official Department of the Army position, policy, or decision, unless so designated by other documentation.

19. KEY WORDS (Continue on reverse side if necessary and identify by block number)

enthalpy-entropy compensation; hydrophobic free energy; polypeptides; protein dynamics; universal exponent; structure/function

20. ABSTRACT (Continue on reverse side if necessary and identify by block number)

A relationship is derived between the thermodynamic entropy-enthalpy compensation of proteins and hyperbolic dynamics of their resting, signal-sensitive behavior. This formulation is then used to derive a hydrophobic sequence code which successfully predicts structure and function in a variety of polypeptide hormones.

DD FORM 1 JAN 73 1473 EDITION OF 1 NOV 65 IS OBSOLETE

UNCLASSIFIED
SECURITY CLASSIFICATION OF THIS PAGE (When Data Entered)

AD-A175 298

DTIC FILE COPY

In: Koslow, S.H., Mandell, A.J., Shlesinger, M.F., eds.,
Perspectives in Biological Dynamics and Theoretical Medicine,
Annals of the New York Academy of Sciences, 1986.

GEOMETRIC UNIVERSALITY IN BRAIN ALLOSTERIC PROTEIN DYNAMICS; COMPLEX HYDROPHOBIC TRANSFORMATION PREDICTS MUTUAL RECOGNITION BY POLYPEPTIDES AND PROTEINS

Arnold J. Mandell, Patrick V. Russo, and Barbara W. Blomgren
Laboratory of Biological Dynamics and Theoretical Medicine
University of California, San Diego
La Jolla, California 92093

Studies of the dynamics of several brain enzymes and membrane receptors indicate that the presence of hierarchical modes in power law spectra is associated with the capacity for signal-sensitive conformational transitions. When transient, this transition to differentiability is characteristic of the system in action; when long-lasting, the mode locked periodicity leads to receptor protein denaturation and desensitized preparations.[1–3] Multiplicity in substrate-velocity curves (iterative saturation plateaus) of allosteric proteins demonstrated comparable multimodality in velocity, V, across increasing substrate concentrations, S, in a staircase of half-maximal rate constants in addition to adaptive renormalization as many smaller steps became fewer larger ones when the concentrations of regulatory ligands, r, were varied (Fig. 1).[3–5]

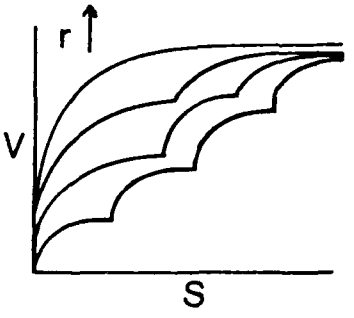

Fig. 1 Ligand-induced renormalization of iterative substrate saturation plateaus in catalytic velocity of allosteric proteins.

We note the loss of multimodal complexity in enzymatic and receptor function away from a quadratically maximal value of r. The problem involves understanding both structural stability with respect to the underlying equations (not initial values) and phase transitions in these dynamical hierarchies. Evolutionary selection of restricted ranges of biological parameters removes genericity, density, or even positive measure as necessary to such explorations. For example, our theory says that the signal-sensitive allosteric protein lives in the ϵ-neighborhood of some complex boundary on the hyperbolic plane. In real parameter space, these are the irregular border regions of competing attractors demonstrating homoclinic tangencies and self-similar scaling.

A Thermodynamic Law for Signal-Sensitive Proteins

The universality of linear free-energy relationships between 250 and 315°K of both rate and equilibrium constants for a wide range of water-solvated organic chemical reactions,[6] including enzymatic catalysis and protein ligand binding[7] by biological macromolecules is seen in the form of a normalizing factor called compensation temperature, α, which rescales the temperature at which a class of reactions are run, leaving invariant the slopes of the linear Gibbs free energies of interaction. α has also been called the isokinetic or iso-equilibrium temperature because Arrhenius or Van't Hoff plots intersect at $1/\alpha$ when temperature compensation is present. The molecular mechanism underlying

those findings, observed most systematically in studies of the effect of aliphatic substitution on ionization rates of organic acids using the Hammett equation, has been called the hydrophobic effect.[8] Water adjusts its geometry to maximize the number of intact hydrogen bonds with itself to neutralize the unbonded electron pair of oxygen by forming clathrate-like convex cages around flickering aggregates of self-seeking, non-soluble organic moieties while in a dynamical struggle to minimize lost solvent entropy. The hydrophobic effect, a function of the aqueous surface ($\sim l^2$), scales the mass ($\sim l^3$) of coherent aggregates of polypeptide polymers as $m^{2/3}$. This estimate has been confirmed in more than 30 proteins up to 50,000 Daltons.[9] The hydrophobic effect as a hyperbolic interfacial free energy scales self-similarly across the hierarchies of peptide clusters in water reflected in the fractional exponential renormalization of their temperature-dependent kinetics. In addition, the isomorphism of their scaling exponents in Euclidean space $\mathbf{R}^2$ and complex space $\mathbf{C}$, x-ray crystallographic and density-of-states spectra respectively (see below), is consistent with a thermodynamic rather than a physical anatomy of these macromolecules.

Water's unusual propensity for dynamical self-rearrangement into states that are both attractive and repelling eliminates negative values for the Gibbs free energy of conventional equilibria. Decomposition of the flow into stable and unstable manifolds makes rigorous thermodynamic treatment inapplicable. That $\Delta G \geqslant 0$ in aqueous solutions of small as well as polymeric organic molecules can be called enthalpy-entropy compensation; $\Delta H = \alpha \Delta S + \Delta G_\alpha$ implies that in the neighborhood of temperature T°_α, ΔH is paralleled by α-renormalized ΔS, leaving the free energy change ΔG negligible and almost independent of the temperature. Using the second-law relationship, $\Delta G = \Delta H - T^\circ \Delta S$, we can rewrite the expression of enthalpy-entropy compensation to demonstrate the role of factor α with respect to the linear free energy as $\Delta G_{T^\circ} = \Delta H(1 - T^\circ/\alpha) + T^\circ \Delta G_\alpha/\alpha \sim 0$. Using estimates of interfacial free energies from surface area and microcalorimetry, calculations of the countervailing forces of water hydrogen bond strain minimization by protein hydrophobic packing and equivalent loss of polypeptide chain entropy in, for example, hen egg white lysozyme ($\Delta G = 350$ kcal $(\Delta H) - 350$ kcal $(T^\circ \Delta S) = 0$) exemplify the way protein dynamics mirror the hyperbolic stability of aqueous solvent.[9] Thermodynamic intuition dictating the axiom of choice based on the variational principle of energy minimization is replaced by one of geometric limits on the maximization of hyperbolic pressure on a quadratic real or complex manifold.[10] Allosteric proteins rest on separatrices between basins of attraction, hierarchically scaled, competing states of hydrophobic aggregation and maximum possible chain entropy with well documented correlation times stretching from 10^{-12} to 10^{3+} seconds.[3] One can, for example, visualize the hierarchically self-similar, homoclinic orbits and/or horseshoes that constitute the strange point sets of Poincaré, Birkhoff, and Smale. The transient global $C^0 \rightarrow C^{\geqslant 1}$ transition to smoothness represents the making of functional connections between elements of the hierarchical machinery. This C^0 resting, sensitive condition stabilizes against the spontaneous emergence of $C^{\geqslant 1}$, coherent biological actions without the appropriate signal. On $\mathbf{C}$ this boundary involves the properties of univalence and discreteness. Signal transduction involves phase transitions to differentiable dynamics followed by relaxation to a previous state of discretely mappable scaling hierarchies. Quantitative universality in macromolecular dynamics arises at the boundary of differentiability on $\mathbf{R}$ and discreteness on $\mathbf{C}$ as a "fixed point." The region of transition can be defined by a unique condition, the presence of iterative roots of a Fibonacci recursion relation, on the embedding of discrete semigroups of nonlinear transformations into continuous ones, $f^n(\cdot) \rightarrow F(\cdot, t):\mathbf{R} \rightarrow \mathbf{R}$ and at a comparable boundary defined by the transformational isometries of Lobachevskii space, $\Gamma(az + b/cz + d):\mathbf{L} \rightarrow \mathbf{L}$.

A continuity in the thermodynamic state space between the two phenomenologically different kinds of water, hydrophobically structured and free, creates the characteristic family of coexistence curves found in the neighborhood of second-order phase transitions. In real space, solvent molecules are interspersed intimately with the amino acids inside globular macromolecules at a ratio of about 3 H_2O:1). The lazy cubic, "sigmoid" kinetic functions of brain enzymes and membrane receptor preparations across changing concentrations of regulatory ligands[11] exemplify the continuous phase transitions of allosteric proteins.

J. Willard Gibbs[12] geometrized the thermodynamic state space of a simple fluid in equilibrium as a once differentiable manifold with the shape of a convex body and a boundary upon which two pure phases, such as hydrophobically structured and free water, meet at a critical point. His phase rule

governing components i, coexisting phases p, and dimensionality d of the manifold M of their coexistence, $i + 2 - p = {}^{\backprime}4^{d} \geqslant 0$, predicts that the pure phases of the protein-water system will meet on a line. A cross-section through this entropy surface creates a two-phase coexistence manifold. At critical values of the parameters, a hierarchy of metastable states emerges in the neighborhood of the critical point, here represented by two descriptions for the same set, superstructured free and superfree structured water as extensions of convex coexistence surfaces (Fig. 2). A Gibbs-like plot of a cross-section through the concave entropy surface diagrams how correlation length diverges with proximity to the critical point in continuous phase transitions,[13] creating a geometrically proportional, dilation symmetric hierarchy with universal scaling exponents of the sort observed in the relaxation spectra of proteins.[3]

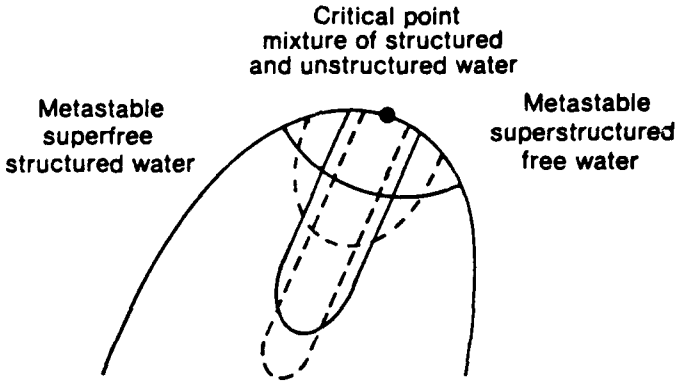

Fig. 2 Correlation lengths along the hierarchies of convex co-existence surfaces diverge near the critical point.

The intrinsic geometric structure of $\mathbf{R}^2$ in interaction with a system having cycles of many orders creates such orbital complexity that its description often requires Markoff partition, symbolic dynamics, and invariant measures such as topological or measure theoretic entropies.[14] Physical (geometric) intuition is lost as the price for quantitative characterization. Although the complicated behavior is generated by deterministic equations, its description in entropies leads to even less insight about the mechanism than the assumptions of a describably constrained but purely random process such as a self-avoiding walk. The focus on "sensitivity to initial conditions" and "rate of information loss" has generated nihilism about a physical understanding of the kind of hierarchical dynamics that characterize the behavior of signal-sensitive proteins.[1] Perhaps consideration of manifolds with other intrinsic geometries will be more rewarding. For example, a global property of aqueous solvent such as its hydrophobic, hyperbolic pressure can be represented as a general characteristic of the thermodynamic manifold, its curvature.

A Natural Metric for the Critical Dynamics of Allosteric Proteins

The intrinsic geometry of the manifolds of thermodynamic minima manifests positive constant Gaussian curvature, $K > 0$; a recurrent orbit has smaller circumference, c, than it would have on the Euclidean plane $\mathbf{R}^2$ (Fig. 3a). In the neighborhood of a stable manifold of an orbit with expanding as well as contracting eigenmotions, the hyperbolic Lobachevskii space L with constant negative curvature, $K < 0$, stretches c beyond its length on $\mathbf{R}^2$ so that for small r its dependence on radius r deviates from $2\pi r$ like $c(r) = 2\pi r - \pi/3 \cdot Kr^3 + \epsilon r^3$ in which $\epsilon \to 0$ as $r \to 0$ (Fig. 3b).

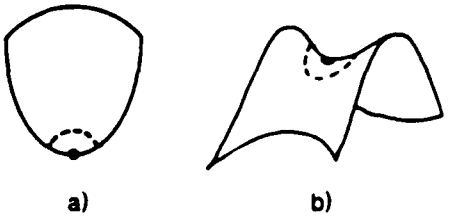

Fig. 3 Manifolds of positive (a) and negative (b) Gaussian curvature.

This phase space (Fig. 3b) can be represented by Lobachevskii's geometry defined by replacement of Euclid's fifth postulate about parallel lines as seen in a construction (Fig. 4) where *two* lines (here symmetric) through points P,P' lie parallel to the given line A,A', separated by their angle of parallelism $\phi = f(r)$ lying between the limit lines of those contained in ϕ that converge to A,A' at infinity. In L space the "equal" distances E,E' and E',E'' between parallel lines A,A':B,B', C,C' appear to shrink at a geometrically proportional rate dependent on $|r - r_0|$, r_0 being in an $\mathbf{R}^2$ neighborhood. A renormalization of this length that is appearing to shrink in geometric proportion along parameter r in $\mathbf{R}^2$ generates metric universality in a geometric series that is uniquely both multiplicative and additive, a Fibonacci recursion relation, $\Phi^n \rightarrow \Phi^{n+1}$... and $\Phi^{n-1} + \Phi^n = \Phi^{n+1}$.

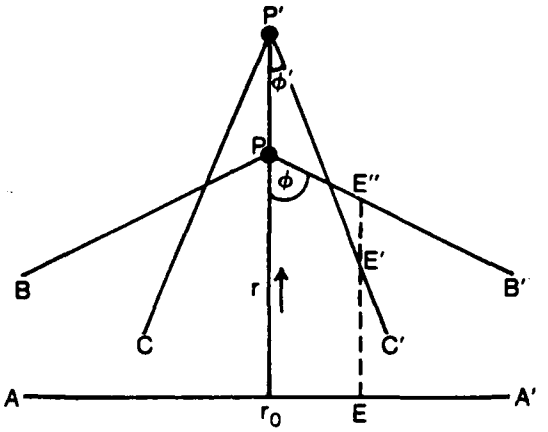

Fig. 4 Lobachevskii's geometry defined by the replacement of Euclid's fifth postulate about parallel lines. See text.

A recurrent orbit in L has length $c \sim \pi l (e^{r/l} - e^{-r/l})$ in which r controls the intrinsic metric of the manifold as in Fig. 4 and l represents an extrinsic unit of length; c grows in a fractionally exponential manner with r. Since $e^{r/l} \sim 1 + r/l + 1/2(r/l)^2 + ...$ and $e^{-r/l} = 1 - r/l + 1/2(r/l)^2 - ...$, $l \sim 2\pi r(1 + 1/6(r^2/l^2) + ...)$, $l = 2\pi r$ only for a small ratio, r/l. The geometric divergence of the metric of L "linearizes" the measure on the geodesics on this manifold, the characteristic behavior of orbits of hyperbolic sets (such as Smale's Anosov-like, non-wandering sets), via fractional linear transformation, Γ. We note that $\phi \rightarrow 0$ and $\mathbf{R}^2 \rightarrow$ L as $r/l \rightarrow \infty$.

A hierarchy of recurrent orbit lengths, $c = f(r)$ in L space can be visualized on the manifold of Beltrami's pseudosphere, Fig. 5, the first geometric realization of Lobachevskii's abstract fifth axiom. It was constructed using a tractrix, a curve whose diameter $\xi \sim |x - x_0| \sim re^{-\alpha}$, is defined by the equidistance of all its tangents to the $x_0 r$ axis which Hilbert proved could not be extended without encountering a fixed-point singularity,[15] in a time-reversed dynamical contraction analogous to the expanding dynamics around the thermodynamic critical point portrayed in Fig. 2.

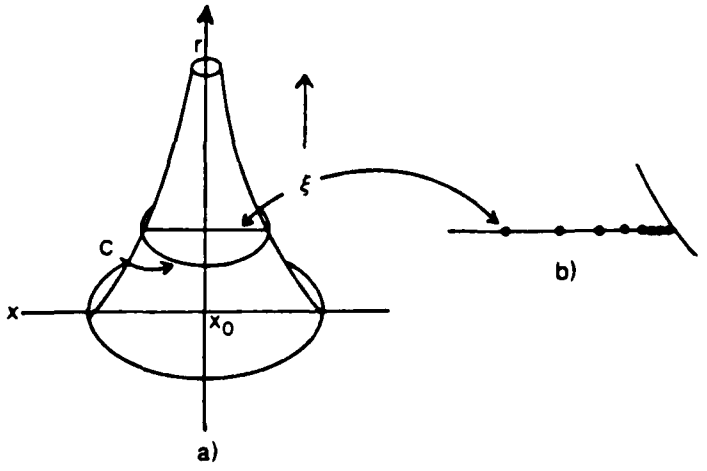

Fig. 5 The normalization of length, ξ, in Lobachevskii space as realized on Beltrami's pseudosphere. See text.

The intrinsic metric of this geometric object representing L space can be demonstrated using a fractional linear transformation Γ which moves across diameter ξ carrying circles into circles and lines into lines in a smooth series of geodesic lengths going as $\xi_{n+1} = (\xi_n + a)/(1 + a\xi_n), |a| < 1$ and dependent upon $K < 0$ of the hyperbolic plane. The r-dependent series, $\xi_0 = a$; $\xi_1 = 2a/1+a^2$; $\xi_2 = \xi_1 + a/(1 + a)$; $\xi = (3a + a^3)/(1 + 3a^2)$... generates points that converge to the endpoint of the diameter as they recede to infinity (Fig. 5b)

Escher's *Circle Limit I* (Fig. 6 left) portrays the geometrically proportional rescaling of the hyperbolic plane in L space when viewed on $\mathbf{R}^2$ as the ratio r/l is extended from its Euclidean neighborhood at r_0. L^{-1} space is seen in Escher's *Smaller and Smaller* (Fig. 6 right) and portrays the opposite kind of scaling series. Again we note that these isometries of L would generate the appearance of physically promising metric universality if treated with renormalization group transformations on $\mathbf{R}^2$.

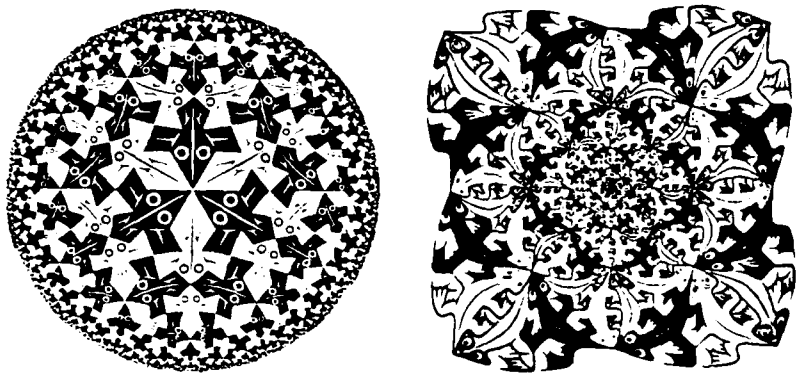

Fig. 6 Escher's *Circle Limit* (left) and *Smaller and Smaller* (right) portraying the intrinsically renormalizing actions of L space.

In hyperbolic L space as a one-dimensional complex manifold with non-Euclidean metric, characteristic of isotopic systems at their critical points (Fig. 1), conformal invariance (angles between any two curves not at vertices remaining unchanged) is demonstrated using fractional linear transformation of the form $\Gamma(z) = az + b/\bar{b}z + \bar{a}$ with $a, \bar{a}$ and $b, \bar{b}$ representing complex conjugate pairs, and $|a|^2 - |b|^2 = 1$. The relation is more easily visualized as $\Gamma(z) = e^{i\alpha}(z - z_0)/(1 - \bar{z}_0 z)$ showing dilation as well as rotation α, the angular derivative $\arg(\dot{z}')$. The distance, d, on a disc in L space from 0 to $r > 0$ using a 1:1 conformal mapping function, $f: L \rightarrow L$, and Caratheodory's classic result that $|f''(0)/f'(0)| \leq 2$ for all geodesic radii (Fig. 7) graphed here as circles (horocycles) orthogonal to $|z| = 1$, is $\int_0^r (2dr/(1 - r^2))$ or, more familiarly, $\log(1 + r/1 - r)$.[16] This is analogous to the Poincaré metric which reduces distances $s(r)$ on L space like $ds = |dz|/1 - |z|^2$ on a manifold of $K = -1$. The renormalization of geodesics on this space of constant negative curvature ($\sim$ Anosov flows) is intrinsic to the metric.

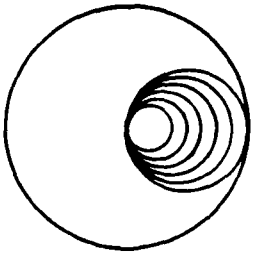

Fig. 7 Horocycle cascade on the Lobaschevskii plane composed of concentrically scaling circular geodesic arcs.

Differentiable Embedding, Iterative Roots, and Mode-Scaling Universality in Allosteric Proteins

Universality in L space can be sought in the form of conformal invariants using their extremal properties. If $f:L \rightarrow L$ defines a homeomorphic conformal map of the unit disc to the open disc which is normalized as in the above, $|f'(0)| = 1$, there is a least upper bound (and greatest lower bound) of the radii, $r_i, r_{i+1} = r_i e^{-\alpha}$, which has been estimated by Bloch[17] to be in the range 0.5666 - 0.65647 in order for distinct transformation, f_i, to achieve distinct values at their centers (univalence). Viewing $f:L \rightarrow L$ as a shift transformation in a one-dimensional dynamical system on the complex hyperbolic plane, contact can be made with comparable quantitative universality at analogous thresholds for the change in character of topological conjugacy functions at this boundary in other one-dimensional dynamical systems.

Our theory is that the phase transition of protein dynamics from resting sensitivity to coherent action consists of a reversible embedding of a hierarchically discrete into a continuous, one-parameter group of transformations, $C^0 \rightarrow C^{\geq 1}$ in **R** and **C**, $f_r^n(\cdot) \longrightarrow F_r(\cdot, n)$. We use the criteria of the existence of the mth iterative root g (for every natural number m, $m > 1$) for the mapping of g such that $g^m = f$ for this embeddability in order to reach another estimate of mode scaling exponent α.[18] Except for the identity $g^m = I$, the existence of iterative roots is rare, so the argument requires the assumption of the evolutionarily selective restriction to a unique neighborhood in parameter space more characteristic of biological dynamics and not the genericity implicit in a theorem. For example, the iterates of g are the functions g^n such that $g^{n+1} = g_0 g^n$ and for $m \leqslant 2$, g is an iterative root of order m of g if $g^m = f$. Using combinatorial methods, it has been proved that the quadratic polynomial defined on the complex plane, $g(g(z)) = az^2 + bz + c$, has no iterative roots[19] and therefore cannot be the form of the resting state with the discrete-continuous embedding property required by allosteric proteins.

In a parameter range of measure zero, a contrasting quadratic transformation on the real line demonstrates the iterative roots (factorization) required for embeddability: geometrically proportional fractional scaling of the expanding modes, the convolutionarily self-similar series $\Phi^n \cdot \Phi \rightarrow \Phi^{n+1}$... such that $\Phi^{n-1} + \Phi^n = \Phi^{n+1}$. Iterative roots, i.e. (acyclic) solutions to Abel's functional equation $\psi[f(x)] = \psi(x) + 1$,[18] exist for $x = \Phi$ because $\psi(\Phi^2) = \psi(\Phi) + 1$, $\Phi^3 = \Phi^2 + \Phi$ ...

Beyond values for r that generate subharmonic bifurcations, the quadratic map on the real unit interval, $f_r:R \rightarrow R$, $[0,1]$, $f_r(x) = rx(1-x)$, reveals its first periodic points not a power of two at $r \geqslant 3.57$.[20] In parameter regions $3.56 < r < 4$ there is an infinite number of periodic points along with loss of diffeomorphic conjugacy (Sarkovskii Theorem, 1964). At $r = 3.83$ numerical analyses reveal a period three whose points are distributed as an isosceles triangle (72°, 72°, 36°) on the quadratic manifold which, after complexification on the half-plane Im $Z > 0$ and fractional linear transformation Γ onto the boundary of the unit circle, the disc in the Poincaré metric, is an isometry equivalent to a rigid rotation (Fig. 8a). The sides are in ratio $AC/AB = (\sqrt{5}-1)/2 = 0.618...$

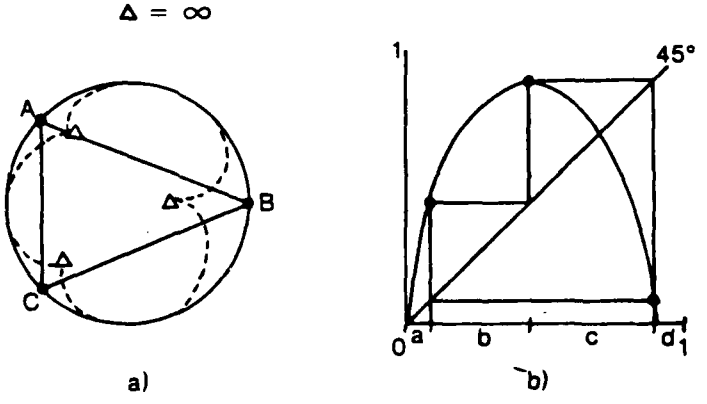

Fig. 8 Period three of the quadratic map on the unit interval distributes like an isosceles triangle on the unit circle with the Fibonacci relation between longest and shortest sides (a); periodic points as the trace of the transition matrix collect as a Fibonacci series (b). See text.

As a subshift of the shift map on two symbols at $r = 3.83$ (Fig. 8b), symbolic dynamics show that regions b and c represent a non-wandering, closed invariant set. When $A = \begin{pmatrix} 0 & 1 \\ 1 & 1 \end{pmatrix}$, representing the b and c transitions, is exponentiated, we have $\begin{pmatrix} 1 & 1 \\ 1 & 2 \end{pmatrix}, \begin{pmatrix} 1 & 2 \\ 2 & 3 \end{pmatrix}, \begin{pmatrix} 2 & 3 \\ 3 & 5 \end{pmatrix}, \begin{pmatrix} 3 & 5 \\ 5 & 8 \end{pmatrix}, \begin{pmatrix} 5 & 8 \\ 8 & 13 \end{pmatrix} \ldots$ Tr(A), the sequence of sums of the diagonal entries, collects finite forward orbits that grow in length in the Fibonacci recursive relation of geometrically proportional numbers converging to $0.618\ldots = \Phi^{-1}$.[21] The transformations $(g = \Phi^n \rightarrow \Phi^{n+1})^m \rightarrow f$ are self mappings g such that $g^m = f$ and g is the mth iterative root which exists for every natural number m as in a sequence of geometric means, $M = \left[\prod_k^m a_k\right]^{1/m}$. This factorability defines the capacity for embedding, $C^0 \rightarrow C^{\geq 1}$, discussed in the context of the dynamics of allosteric proteins.

Consonant with the location of the fixed points on the boundary (Fig. 8a), the invariant open set complementary to the closure of the forward orbit of these critical points is an expanding dynamical system.[22] Remove these three fixed points from the invariant manifold, and everything between them becomes negatively curved into the natural hyperbolic Lobachevskii space of the $C^{\geq 1}$ functioning system (Fig. 8a).[23] The embeddable hierarchy with iterative roots is C^0, the discrete signal-sensitive resting condition, represented by Fibonacci rotations Φ^n on the boundary, and the expanding hyperbolic, structurally stable system within the domain of the non-Euclidean metric is the manifold of transiently coherent protein action.

A Generalization of the Unique Geometric Universality of the C^0, $C^{\geq 1}$ Boundary

(a) From the point of view of ergodic theory, the unit circle is the same as the unit interval. $f{:}R \rightarrow R$ defined by $f_\omega x = x + \omega \pmod 1$ is the fractional part of $x + \omega$ on [0,1] as it is in a rotation of angle θ on $z \in C, |z| = 1$, $f{:}S^1 \rightarrow S^1$ defined by $f_\omega \theta = e^{i2\pi(\theta+\omega)}$. If ω is rational f_ω is finitely periodic; if ω is irrational the point set resulting from the iterative composition of expanding map f covers the whole line. The two-parameter *nonlinear circle map* with a quadratic maximum, $f_{r,\omega}{:}S^1 \rightarrow S^1$, defined by $f_{r,\omega} = \theta + \omega - r/2\pi \sin 2\pi\theta$, locates the boundary of the isometries defined by fractional linear transformations Γ of L space. Poincaré defined the rotation number for a homeomorphic map on the circle S^1 as $\rho(f_{r,\omega}) = \lim_{n\rightarrow\infty} (f^n(\theta) - \theta)/n$, and at the limit of topological conjugacy, $r = 1$ and $\rho(f) = 0.618\ldots$[24,25,26] The power spectrum of the critical map, the "universal spectrum" at $r = 1$, scales like $S(\omega) \sim -\alpha^{-1}S(\alpha\omega)$, $\alpha = 0.618\ldots$

The unit circle can be suspended as a torus, and then dividing the torus by an involution $f(z) \rightarrow -Z$ ($T^2 \rightarrow S^2 \rightarrow D^2$) yields a hyperbolic L-manifold with metric scaling properties as a function of $|r_c - r|$ (Figs. 3 - 6).[27] At high nonlinearity the crinkled circle of numerical studies of critical maps on R^2 demonstrates similar hierarchies before loss of topological conjugacy [28]. A quantitative similarity between the Bloch constant estimate on the limit of univalence of one-dimensional dynamics on L and topological conjugacy of the nonlinear circle map on the boundary of L space is suggested. The Jordan curve resulting from the limits of the ϵ-perturbation $z \rightarrow z^2 + \epsilon$ (Fig. 9) is the same quasicircle observed with critical nonlinearity of $f_{r,\omega}$. With $\hat{\rho}(f)$ irrational, the dynamics compose an invariant minimal set, perfect and homogeneous, which is either S^1 or a Cantor set at $r \geq 1$.[29] The irrational $\hat{\rho}(f)$ of "the last torus to go" inscribing the universal spectrum with scaling exponent (winding number) $\alpha = 0.618\ldots$ and continued fraction expansion [1,1,1,1...] can be related to the Bloch constant limit on the modular radii of univalent transformations Γ via the well known relation between $\Gamma(z) = az + b/cz + d$ and continued fractions [...] which can be used to expand $\hat{\rho}(f)$: if $\hat{\rho}(f)_i \rightarrow [n_1, n_2 \cdots]$ and $\hat{\rho}(f)_j \rightarrow [m_1, m_2 \cdots]$ then $\hat{\rho}(f)_i = \Gamma\hat{\rho}(f)$, if there exist k, l such that $(-1)^{k+l} = 1$ and n_{k+r} and m_{l+r}, for $r \geq 0$.[30]

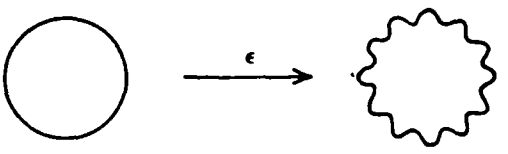

Fig. 9 When $z^2 \rightarrow z^2 + \epsilon$ the unit circle becomes an unrectifiable Jordan curve whose Hausdorff dimension varies continuously as ϵ^2.[33]

(b) The one-dimensional dynamical system on complex space comparable to the logistic map on the reals $f_r: \mathbf{C} \rightarrow \mathbf{C}$, $f_r(z) = rz(1-z)$, or its conformally equivalent $z \rightarrow z^2 + \epsilon$, manifests the same renormalizable geometry on $\mathbf{R}^2$.[31] Its expanding property with respect to both hyperbolic stretching of the manifold (Fig. 3b) and the role of critical loss of rectifiability can be seen in comparing the undecomposable continuum of orbits of the unstable homeomorphism $f(z) = z^2$,[32] with absolute derivative two and topological dimension one with its perturbation to a Jordan curve (Fig. 9a,b) by $f(z) = z^2 + \epsilon$. As ϵ grows further, the set has topological dimension one, linear Lebesgue measure zero, and positive Hausdorff dimension d_H, indicating that the density scales as radius r^{α} with $d_H \sim 1 + \epsilon^2$.[33] The Hausdorff measure transforms analogously to the conformally equivalent Lebesgue measure, μ, $f^*\mu = |f|^2\mu$ in the form $f^*\mu = |f|^p\mu$. Recent numerical simulations of the interior of the Mandelbrot bifurcation set of $z \rightarrow z^2 + \epsilon$ (H-O. Peitgen, personal communication, 1986) demonstrate that in going to the boundary d_H ranges from 1 to 2 (in parameter space) and loses topological conjugacy at a radius with respect to the boundary which, estimated from the computer graphic display, is $\sim$ 0.62. This may represent a numerical way to sharpen the range of the Bloch constant estimate on univalence.

(c) The earliest demonstration of the geometric origin of the universal boundary between C^0 hierarchical complexity and $C^{\geq 1}$ analytic expansions (or contractions) on $\mathbf{C}$ and therefore on $\mathbf{R}^2$ was the first proof of the boundary of disjointness as a mode-scaling invariant in $\mathbf{C}$ or $\mathbf{R}^2$ (0.618...2/3) by Cayley.[34] He used only the constancy of the ratio of distances of imaginary points a_i on any circle to any two antipoints n, n' on a common indefinite line and the doubling of the angle between them associated with convergence in the geometric series, $a_1 n/ka_1 n'$, $a_2 n/k^2 a_2 n'$, $a_3 n/k^4 a_3 n'$... to prove a sufficient but not necessary condition on the "bad set" in the modulus of the difference between two complex quantities, mod. $(z_i - z_j) < 2/3$ mod. z_j, for the regular convergence "of any initial point taken at pleasure," $z_i \rightarrow z_j$, solving $(z_i + h)^2 = z_j^2$ as $h \rightarrow 0$ by iterating the Newton-Fourier algorithm $z_1' = (z_i^2 + z_j^2)/2z_i$, z_2'... He showed that with initial values in the "unfit segment," long irregularly behaving transients could (but would not necessarily) occur before the eventual convergence to the attractor's fixed point. This appears to be one of the first descriptions in the literature of the fractal set at the mutual boundary of basins of attraction.[35,36] In this context the quantitative issue becomes one of estimating the normalized size of the conformally invariant, non-complicated domain between the basins of attraction of the roots of a complex quadratic polynomial, the normal set of Fatou. The implication is that the unstable fixed points ($\sim$ the Julia sets) which generate fractal basin boundaries analogous to those found, for example, in nonlinear second-order maps on the reals,[37] are complementary to expansive transformation groups with emergent geometric rigidity such as invariant d_H occurring at a critical distance from the Euclidean approximation as the forward orbits escape to infinity (Figs. 4 and 5).[38] The unstable critical points of the Fibonacci recursion seen in the logistic map at $r = 3.83$ in $\mathbf{R}$ (Fig. 8b) can be identified with the closure of the repelling periodic points of the Julia set in $\mathbf{C}$.

(d) Another way of generating hierarchies at the C^0, $C^{\geq 1}$ boundary includes the Hardy-Weierstrass trigonometric map, $f: S^1 \rightarrow S^1$, defined by $f_{\gamma\lambda} = \gamma^{-n} \cos(\lambda^n t)$ with the Hölder exponent serving as the bound on differentiability, $\log \gamma^{-1}/\log \lambda = 1$.[39] We note here that $(0.618...)^{-1} = 1.618...$ uniquely. A generalization of this lacunary power series, a transformation of the cycles of all orders analogous to that seen in the logistics map at $r = 3.83$,[40] $\sum_1^{\infty} a_i z^{n_i} (n_{i+1}/n_i \geq k > 1)$ with equivalence of its Hausdorff and spectral dimensionalities has been called a perfect set of unicity and multiplicity.[41] We shall see below that this relation is realized in physical studies of proteins. A critical level of competition between convergent, γ, and divergent, λ, motions in these trigonometric maps of hyperbolic orbits in thermodynamic phase space represents the forces of hydrogen bond maintenance versus solvent entropy preservation and polymeric aggregation versus chain entropy maximization constituting the hyperbolic pressure of allosteric proteins in solution. This dissipative yet area-preserving dynamic in $\mathbf{R}^2$ can be represented most simply by a hyperbolic linear map $f(x) = Ax$, $A = \begin{pmatrix} \lambda & 0 \\ 0 & \gamma \end{pmatrix}$, $0 < \gamma < 1 < \lambda$, and $\det A = 1$. A single parameter, derived from the sequence of amino acids in peptides as hydrophobicities, determines the hyperbolic pressure of proteins defined as $r = (|\lambda| - |\gamma|) > 0$, $(\lambda + \gamma) = 0$ (see below).

A simple construction (Fig. 10) generalizes the role of the critical balance of the components of hyperbolic pressure around $\lambda + \gamma = 0$ as the expanding and contracting manifolds of a one-parameter group of transformations in $\mathbf{R}^2$ or $\mathbf{C}$, which is analogous to the steepness (or height) of the quadratic manifold of Fig. 8b. It demonstrates the geometrically invariant self-similarity of the critical boundary between the C^0 and $C^{<1}$ global (not local) conditions. In the near-critical case when $\lambda + \gamma < 0$, Fig. 10 shows three lines with a diminishing series of segments with ratio $1/\Phi$ that have the unit of measure as the first term: AB = BC + CD, BC = CD + DE...and AB/BC = BC/CD = CD/DE... = Φ. $f^{\theta}_{90°}\mathbf{R}^2 \rightarrow \mathbf{R}^2$, leads to a series of lines at equal intervals, θ, (like time) radiating from the pole (fixed point).

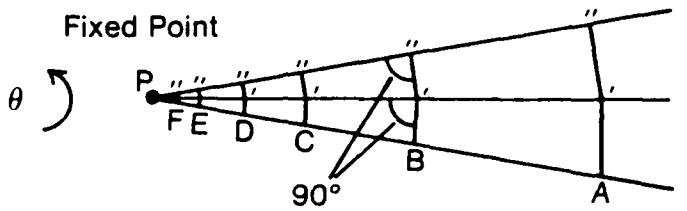

Fig. 10 A one-parameter group of transformations, $f^{\theta}_{90°}$, generates Fibonacci scaling at the boundary of differentiability. See text.

The self-similarities intrinsic to geometric progression abound. The triangles PAA' and PA'A" are similar, since the corresponding angles are equal. On these grounds, PA'/PA = PA"/PA'..., and the lengths PA, PA', PA" constitute a geometric series. The triangles PBB', PB'B"... are part of the same series of triangles, and PB, PB', PB" compose terms of the same geometrical progression. Of course PA, PB, PC... form a geometrical progression, for they are "equally spaced" terms of the one just mentioned (see Fig. 4). Another geometrical progression is formed by the lengths AA', A'A",...BB', B'B"... The quadrilaterals AA'B'B, A'A" B"B'... are all similar since they have equal corresponding angles and pairs of sides in proportion.

Although this construction begins with the one parameter being the perpendicularity of the A → A', A' → A" lines intersecting with the radii, a Fibonacci recursion of radial lengths would have emerged naturally from f^{θ} if the parameter (instead of sequential 90° interactions) was the restraint that PA, PA', PA" be in geometric progression. In the same way, the problem of determining an infinite number of countable intermediate points reduces to that of finding the geometric means, $M = \left(\prod_k^m a_k\right)^{1/m}$, between the lengths of existing radii PA,PA'... These one-parameter homothetic transformations put the iterative-root, embeddability theorem[18] relating the geometrically singular condition on the common boundary between discreteness and continuity in expanding (or contracting) maps of the plane in the context of Ahlfors's "ultrahyperbolic" Poincaré metric in L space with Gaussian curvature $K = -1$ via conformal invariance.[27] The elements of the group $\Gamma(z) \subset L$ are conjugate to $f^{\theta}_{90°}(x,y) \subset \mathbf{R}^2$ on the geometric space of Fig. 10. Both contain the action of renormalization as an intrinsic feature of the geometry of their manifolds; both are transformationally invariant with respect to translation, inversion, rotation, and dilation.

If in Fig. 10 the sequence of radii from circle center P, PA, PA', PA"... were not in geometric ratio, but PA/PA' = PA'/PA" = 1, the triangles PAA' and PA'A" as well as their nested, self-similar convergence PBB', PB'B", PCC', PC'C"... would satisfy the strong triangle inequality d(PA) = max d (PA') ≥ AA'). This generates a sequence of isosceles triangles that serve as a condition on the boundary of individual clusters in hierarchical structures as defined by relative nearness on a topological space.[42] This boundary, then, defines the limit of disjointness in ultrametric spaces, hierarchical lattices like corporate tables of organization or upside-down trees. This topology with the common currency of time has been used to relate the stretched exponential relaxation of hierarchical dynamics (the characteristic function of the fractional power law scaling spectra of Lévy, convolutionarily self-similar distri-

bution laws[43]) and random walks on hierarchical manifolds.[44,45] Isomorphisms of the Lévy mode distribution are generated by the Hardy-Weierstrass cosine series [39] as well as the Salem sets of uniqueness and multiplicity[41]; at their boundaries, both demonstrate the nested property of the strong triangle inequality of ultrametric spaces and the iterative roots (like self-similar Lévy convolutions) of embeddable maps at the C^0, $C^{\geq 1}$ boundary.

In passing we note that in the critical neighborhood of $\lambda + \gamma > 0$, $PA/PA' = PA'A'' > 1$ such that angles similar to $B'AA' = 90°$ (rather than those similar to $B'A'A = 90°$ in Fig. 10), a similar geometric proportionality with embeddable scaling Φ bounds the radii from the other side, i.e. with cords similar to AA' normalized to 1,the radii are equal to Φ and will grow both additively, $\Phi^{n+1} = \Phi + \Phi^n$, and multiplicatively, $\Phi^{n+1} = \Phi \cdot \Phi^n$ in a manner characteristic of this unique geometric progression. With the strong triangle inequality of ultrametric spaces, topological hierarchies are bounded on both sides by the geometric scaling of the Fibonacci recursion relation. Since this boundary has measure zero, the apparent diversity in descriptors may be regarded as identities. A related treatment of the boundary of probabilistically disjoint spheres bounded by imaginary quadratic irrationality, which can be represented by periodic continued fraction expansions and contains logarithmic density distributions of geodesic orbits, exploits the hyperbolic metric of Figs. 3 - 6. Sullivan's theorem[46] that the universality of this boundary on disjointness comes from a one-dimensional reduction fits both Hamiltonian dynamics when studied on a circle and the three-parameter Cartwright-Littlewood equation when examined on the plane (see below). Fig. 10 portrays the underlying geometric universality at the border of differentiability in $\mathbf{R}^2$ and C that has emerged from a variety of formalisms, including the renormalization group transformation of distances as the critical point is approached. Whether this measure zero boundary looks fractal or smooth depends on the point of view of the observer.

A Differential Equation for the Thermodynamics of Signal-Sensitive Proteins

Through nonlinear positive and negative dampening, the r-parameter of the Cartwright-Littlewood, van der Pol equation[47] regulates the global hyperbolic mechanism of the flow at the C^0, $C^{\geq 1}$ boundary; the critical value of the normalized amplitude parameter is $b \geq (\Phi^{-1} - 2/3)$. This global property represents the competing components of the hyperbolic stability of allosteric proteins in water. The system at $r > r_c$ can be regarded as an expanding dynamical system, analogous to a polynomial vector field in $\mathbf{R}^2$ in x and y when studied at high nonlinearity.[28] Differentiating $f(x) = \ddot{x} - r(1 - x^2)\dot{x} + x = rb \cos \lambda t$ and rescaling, $\dot{y}/r \rightarrow y$, leads to the pair of ordinary differential equations: $\dot{x} = y - r(x - x^3/3)$ and $\dot{y} = -x/r + b \cos \lambda t$ whose behavior can be examined in phase space as well as on the two-parameter plane. The dimension x portrays hydrophobic packing, ΔH, in the interval [0,1] and y, the entropy, $T°\Delta S$, normalized in the same way. Fast hydrophobic aggregation followed by the slower rearrangement of hydrogen bond cages makes the relaxation oscillations of this equation set realistic. Because both properties are tightly linked (are, in effect, two aspects of the same thermodynamic motions), the behavior can be viewed as x versus $\dot{x}$ trajectories in one-dimensional dynamics on a two-dimensional phase plane. The parameter λ signifies the complex hydrophobic mode of a polypeptide transmitter or ligand, the normalized external "driving" signal is $\cos \lambda t$; b serves as the amplitude parameter of the driving force representing the amount of transmitter/ligand message which we use in a pharmacological "dose-response" fashion to investigate the geometric universal scaling relation at the boundary of differentiable mode-locking behavior. The physical exchange between polypeptide transmitter and protein receptor is in the form of interfacial surface tension generated by their mutual hydrophobic attractive forces which are 100× greater than predicted by van der Waal theory and extend up to 10 nanometers, the size of a neuronal gap junction.[48]

At $b = 0$, numerical analyses of this system showed that increasing hydrophobic, hyperbolic pressure r stretches the manifold of the unperturbed relaxation oscillator (Fig. 11a) and slows its native frequency in a nonlinear manner (Fig. 11b).

Power spectral transformation as a density-of-states spectrum over increasing hyperbolic pressure parameter r is qualitatively 1/f, and a deconvolution generates the characteristic stretched or algebraic correlation function of hierarchical dynamical structures. It is of more than historical interest that van der Pol's original diode-rectifier circuit[49] manifested an r-dependence of the relaxation times τ_i that varied as $\tau_{i+1}/\tau_i \sim \Phi r/\omega_0^2$. Here $r/\omega_0^2 = RC$, and emf-driven RC circuits model the dynamics of ion-conductance behavior of allosteric membrane proteins very well.[50]

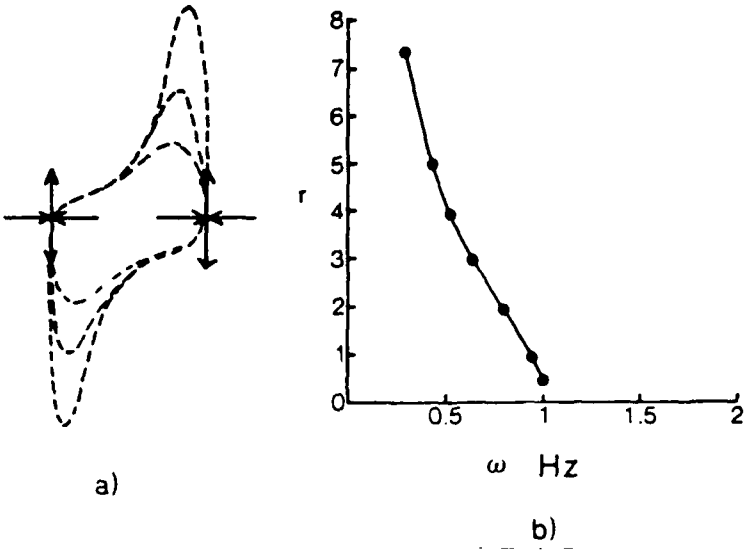

Fig. 11 An increase in hyperbolic pressure parameter r stretches the manifold (a) and slows the frequency (b) in the unforced Cartwright-Littlewood attractor.

The characteristic influence of an increase in hyperbolic pressure $0.5 < r \leqslant 1.5$ on the periodically transmitter- or ligand-driven system, $b > 0$, with λ held between the Arnol'd tongues[51] of mode-locked winding numbers can be seen in Fig. 12, left versus right. As might be anticipated from Fig. 11, an increase of hyperbolic pressure (up to some quadratic limit) increases the complexity between mode-locked tongues in the phase space of the orbital dynamics from which one would predict an increase in some measure of complexity such as the Hausdorff dimension d_H. This leads to the physically counterintuitive prediction that resting (not mode-locked) proteins with higher average amino acid hydrophobicities will manifest higher Hausdorff dimensionality in time and space (see below).

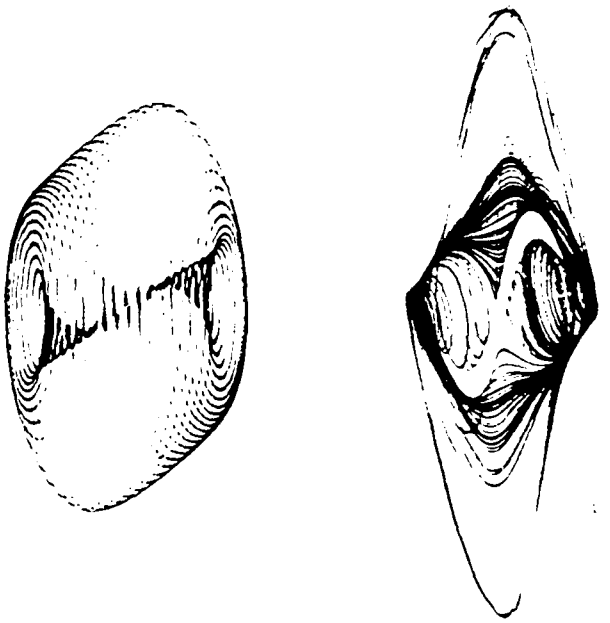

Fig. 12 The Cartwright-Littlewood attractor between mode-locking parameter zones at lower (left) and higher (right) levels of hyperbolic pressure. See text.

The strange dynamics of the periodically driven attractor (Fig. 12b) are controlled by the r-dependent linkage between x and $\dot{x}$ in which the velocity adjusts itself to make the bivalent dampening balance the forcing term, i.e. area-preserving, dissipative forcing. The global hyperbolic pressure generated by $x_0, \dot{x}_0$ repulsion and $x > \pm 1, \dot{x} > 2/3$ attraction is focused at the saddle-sinks where $\dot{x} = 0$

and $x = \pm 1$ (Figs. 11 and 12). They play a determining role like critical points in the region of continuous phase transitions (Fig. 2) and points with characteristic derivative $f'(z) = 0$ when in the limit sets of analytic maps such as $z \rightarrow z^2 + \epsilon$ or the conformally equivalent $z \rightarrow \epsilon z(1 - z)$ (Cvitanovic and Myrheim, unpublished, 1984).[38]

The trajectories speed around the $\dot{x}$ axes, slow critically at the saddle sinks, undergo a periodic "tug-of-war" between leaving and staying which generates whorls of splinter orbits[52] that grow in number tangent to the insets, past the saddle sinks until they get too close to the central repeller $x_0, \dot{x}_0$ and are driven to accelerate toward the next $\dot{x}$ axis and begin again (Fig. 12b). That the complexity arises from the invisible central repeller and the mixmaster-like actions of the two saddle-point repellers between linear segments of the flow is analogous to the dynamics in the neighborhood of the Julia sets in polynomial maps of the complex plane (and unstable fixed points at the fractal basin boundary).[36] Whorls of intermittent "bursts of persistence" have been reported as generic in numerical studies of critical nonlinear maps of the plane.[53] This behavior can be quantified using local escape rates from initial conditions in the neighborhoods of these fixed point repellers.[54] Physically, these critical points represent the extremes of the protein's breathing motions between maximal hydrophobic packing and nearly denaturing entropy gain through unfolding of the peptide polymer.[3]

Squeezed between accelerating repulsion at $x_0, \dot{x}_0$ and dampening contraction at $x > \pm 1, \dot{x} > 2/3$, the dynamics create an annulus on the plane, which although dissipative, is analogous to the area-preserving Birkhoff attractor with different inner and outer rotation numbers, non-trivial intervals between them, and two distinct invariant points.[55] The existence of infinitely many periodic motions near a stable periodic motion as well as motions that are not periodic but are uniform limits on periodic motions follows from the Poincaré-Birkhoff theorem and is seen directly in a variety of these Cartwright-Littlewood attractors (Fig. 12b). Recent numerical studies of a two-parameter family of dissipative twist maps of the annulus (Aubry-Mather sets) demonstrated non-trivial intervals enclosed by the internal and external rotation numbers similar to those seen in the conservative case.[56] Their existence in these innately unstable analog computer simulations of the Cartwright-Littlewood attractor confirms previous observations that these rotation intervals, as studied in digital simulations of dissipative circle maps, are remarkably stable to ϵ-perturbation[57] as well as to random noise. This may justify referring to Fig. 12b as a phase-locked strange attractor (M. Casdagli, personal communication, 1986). It portrays the complex thermodynamic phase-space dynamics of the hydrophobic free energy of signal-sensitive proteins where $\Delta G \geqslant 0$.

The analogy between the behavior of this $f(x)$ in the intervals of rotation numbers on $\mathbf{R}^2$ and that of $\Gamma(z)$ on L is clear. For $\Gamma(z) = az + b/(cz + d)$ with $ad - bc = 1$ and $\Gamma(z)' = (cz + d)^{-2}$, the orbit $\{z \mid |cz + d| = 1\}$ is the isometric circle, c, of $\Gamma(z)$ since $\Gamma(z)$ rescales lengths within it.[27] Or, from another point of view, as in Figs. 4 - 7, $f_r: \mathbf{R}^2 \rightarrow L$ is a transition from a Euclidean to a Poincaré metric at some critical hyperbolic pressure r. This $\mathbf{R}^2 \rightarrow L$ region of transition is the same as that of degenerate Hopf bifurcations.[58] In the L neighborhood, with a surface of constant negative curvature, the orbits have positive topological entropy and the system demonstrates near Anosov structural stability,[59] behavior on an annulus analogous to that of a hyperbolic automorphism on the torus.[60] The implicit analogy with Axiom A flows as the generic hyperbolic sets of allosteric proteins can be argued more easily if we weaken the conditions so that no more than one characteristic exponent is equal to zero, leaving exponential growth and decay of perturbations intact and eliminating the strong uniformity condition which is physically difficult to realize. One can visualize the center manifold of protein actions such as catalysis or binding modulated by transverse hyperbolic macromolecular motions.[3] In the region of geometric proportionality, distance is rescaled via the Fibonacci recursion relation (Fig. 10). This neighborhood of the C^0, $C^{<1}$ boundary is that of the signal-sensitive condition manifested in the universal power spectrum of allosteric proteins. With loss of hyperbolic pressure, $r < r_c$, $f_r: L \rightarrow \mathbf{R}^2$, the topological entropy $h(f)$ goes to zero with the loss of the negative curvature as $L \rightarrow \mathbf{R}^2$.[61] A similar loss of complexity occurs in the (r, λ, b) zone of mode locking on the invariant circle, rational rotations on the boundary c.

Numerical analyses of the Cartwright-Littlewood equation in r, λ space demonstrate at $0 < r < 1.0$ almost the full Farey sequence of winding numbers $\rho(f)_i$ up to a denominator of 9, with $\rho(f)_i$ that appear to be continuously dependent on r, λ, and b. Generally, increasing $r \geqslant 0.5$ decreases parameter space complexity, seen in the progressively lower denominators of $\rho(f)_i$ which increase in size and

decrease in number in a process seen also in the expanding Arnol'd tongues representing the mode locking zones of the winding numbers (1/1, 2/1, 3/1... going from left to right in Fig. 13. With the exception of the 1:1 tongue, the continuous parameter dependence of $\rho(f) = f(r,\lambda,b)$ appears to break down into islands across λ as a function of increasing r and b.

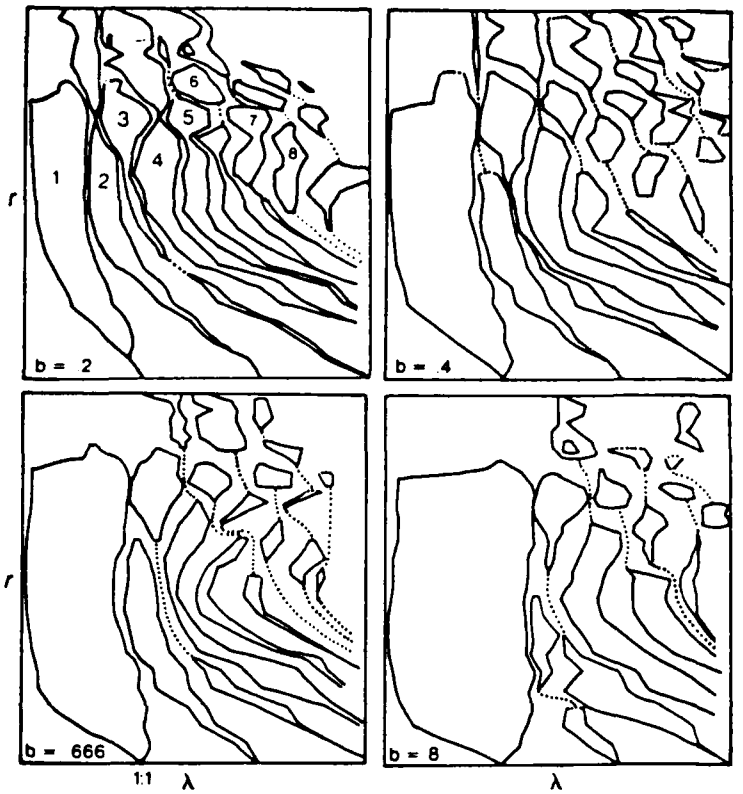

Fig. 13 Mode-locking zones of the Cartwright-Littlewood attractor in $r\,\lambda$ parameter space. Zones of 1:1, 2:1, 3:1, 4:1... are indicated in a dose-response study of the system over increasing b. The 1:1 Arnol'd tongue goes across all of r at $0.666 < b < 0.700$.

Like the existence of non-trivial intervals between internal and external rotation numbers (Fig. 12), at high nonlinearity r the loss of tongues and the emergence of mode-locked islands surrounded by complicated sets (here overlapping of the neighborhoods of at least two $\rho(f)_i$) are reminiscent of the behavior of Hamiltonian dynamics with perturbation-induced destruction of KAM surfaces and the appearance of islands surrounded by Arnol'd diffusive stochasticity in the neighborhood of their separatrices.[25] A third similarity to the results of studies of nonlinear stability in conservative systems is the scaling relation of the invariant circles at the boundary of topological conjugacy (previous section). We see a transition to 1:1 mode locking across all of r in the general vicinity of the driving frequency, amplitude scaling parameter $b \sim 2/3$ as first reported by Cartwright and Littlewood.[47] This scaling, comparable to the mode ratios and power law (Φ, Φ^{-1}) generated by a Fibonacci recursion at the boundary of chaos in standard map models of KAM systems,[25] has been noted previously. Numerical simulation using double precision digital computing will be required to determine the boundary precisely. The mode-locked insensitivity at $b > 2/3$ models the habituation-desensitization behavior of signal-sensitive systems at high levels of transmitters, ligands, or drugs.[2]

A link to the low-dimensional, thermodynamic physics of proteins in aqueous solution can be made from the geometric universality of $(\Phi...2/3)$ on $\mathbf{R}^2$ and $\mathbf{C}$ seen in both dissipatively forced and conservative nonlinear systems to the enthalpy-entropy compensation of critically forced water by recalling that the mode ratio ω_3/ω_1 found in the Fourier transformed velocity measurements made in the Couette-Taylor system (ω_2 was transient) at $r/r_c = 10 - 11$, just before the appearance of the chaotic band, is in the range of 0.62 - 0.65.[62]

Stapleton's Hausdorff Measure and Spectral Scaling Exponent on Allosteric Proteins in $\mathbf{R}^2$ and C

The preceding development leads to four rather straightforward predictions[63,64]: (1) The temperature dependence of the mode scaling exponent of the density-of-states spectrum of allosteric proteins will reflect their hyperbolic, hydrophobic pressure at the limit of the C^0, $C^{>1}$ boundary as a Fibonacci recursion relation; (2) the abstract geometric grounds of these relational constants will lead to experimentally verifiable isometries between $\mathbf{R}^2$ and C; (3) the physical basis of this relational universality is the hyperbolic thermodynamic stability of allosteric proteins in aqueous solution which will be quantitatively related to their complex hydrophobicities; and (4) these measures on the complex hydrophobic dynamics of proteins will be reflected in (all) other proper indices of their thermodynamic structure.[10]

The temperature dependence of the density-of-states spectra in studies of Raman relaxation rates in C of four iron-binding allosteric proteins when compared with ordinary solids was found to be anomalous.[65] The density varied with temperature past both the T^2 and characteristic phonon localization regions of the scattering relation of amorphous solids as γ^{m-1}, and m varied from 1.61 ± 0.05 to 1.67 ± 0.03 (i.e. a complex temperature scaling exponent α of 0.618...2/3). The Hausdorff dimension d_H of the x-ray crystallographic maps of the distributions of the amino acid alpha carbons of these same proteins in $\mathbf{R}^2$ determined via packing density as a function of the radius, mass $\sim r^{\alpha}$, yielded nearly identical values for α.[66]

The hyperbolic thermodynamic stability hypothesis predicts that in contrast to the intuition that amino acid chains that are hydrophobic aggregate to occupy smaller areas of Fourier and Euclidean space, the spectral scaling and Hausdorff mass scaling exponent α would vary *with* the average hydrophobicity per residue using a Tanford-derived set of amino acid hydrophobic free energies determined by their ethanol-water partitions.[67] Table 1 lists six iron-binding proteins for which the amino acid sequences were available. We note that whereas allosteric proteins such as myoglobin demonstrate phase transitions and the Φ scaling of the C^0, $C^{>-1}$ boundary, ferredoxin and putidoredoxin, which are not allosteric proteins, do not.

Table 1

Protein	Avg. Hydrophobicity (kcal) per Amino Acid Residue	ESR (C)	X-ray ($\mathbf{R}^2$)
Myoglobin azide	1.34	1.65	1.65
Myoglobin	~1.34	1.67	1.65
Cytochrome P-450	1.32	1.64	1.63
Ferredoxin	1.11	1.34	1.37
Putidaredoxin	1.21	1.34	1.36
Cytochrome C-551	1.27	1.43	1.50

A structural correlate of the complex hydrophobic, hyperbolic pressure hypothesis is that faster frequency modes and increased spectral and Hausdorff dimension will be reflected as well in increased optical rotatory dispersion as percent helix and related in part to the average amino acid hydrophobicity. For examples: lysozyme with an average hydrophobicity of 1.24 kcal/residue and a dominant mode spectrum demonstrating a 2.5-residue wavelength (see below) has a Stapleton d_H of 1.66 and 35-45% helix; pancreatic ribonuclease, with an average hydrophobicity of 1.02 kcal/residue and a dominant 5.9 and 11.43-residue hydrophobic mode, has a Stapleton d_H of 1.33 and less than 15% helix.[68] Other examples for which data are available on d_H, % helix respectively: myoglobin 1.65, 87.6%; adenylate kinase 1.59, 61.9%; cytochrome C 1.61, 48.5%; lactic dehydrogenase 1.50, 41.6%; carboxypeptidase 1.51, 39.5%; subtilisin 1.46, 32.4%; alcohol dehydrogenase 1.43, 29.1%; papain 1.42, 27.8%; carbonic anhydrase 1.33, 16%; chymotrypsin 1.32, 4.1%; concanavalin A 1.26, 2.5%.

Complex Hydrophobic Transformation of Amino Acid Sequences Predicts Hormone-Receptor Recognition

The dynamics of the Cartwright-Littlewood equation for the transmitter/ligand-driven, enthalpy-entropy oscillations of allosteric proteins with the capacity for signal-induced C^0, $C^{\geq 1}$ transitions predict that hydrophobic mode resonances between polypeptide hormones ($\cos \lambda t$, b) and membrane receptors allosterically regulated by r in a common aqueous field are the source of reversible action-inducing and (if too extreme) irreversible desensitizing phase transitions.

Fourier transformation of the partition coefficients as hydrophobic free energies in kcal/mol[67] representing the amino acid sequences as a time series (Table2)[63,64] generated hydrophobic mode power spectra for polypeptide polymers.

Table 2
Amino Acid Hydrophobicities (kcal)

Ala	0.87	Glu	0.67	Leu	2.17	Ser	0.07
Arg	0.85	Gln	0.00	Lys	1.64	Thr	0.07
Asn	0.09	Gly	0.10	Met	1.67	Trp	3.77
Asp	0.66	His	0.87	Phe	2.87	Tyr	2.76
Cys	1.52	Ile	3.15	Pro	2.77	Val	1.87

For example, Fig. 14 (left) shows the hydrophobic sequence spectrum of the 41-amino acid corticotropin releasing factor (CRF) and five analogues with ~50% amino acid homology but nearly equivalent potency[69] that demonstrate a common dominant mode of ~ 2.1 residues. Fig. 14 (right) shows similar transformation of the 44-amino acid growth hormone releasing factor[70] and several peptides with a variety of different previously designated actions which, although considerably less than 50% homologous with respect to specific amino acids are roughly equivalent in their capacity to release growth hormone from pituitary analog cell preparations (F. Zeytin, personal communication, 1985). All their spectra are dominated by 4.0-residue hydrophobic modes.

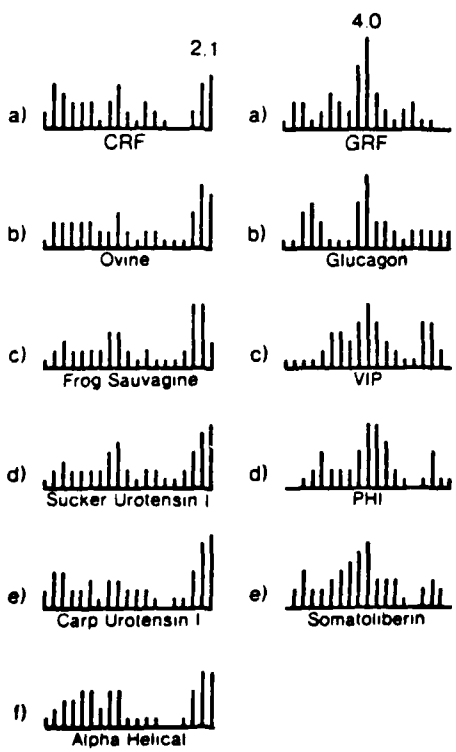

Fig. 14 Hydrophobic mode spectra of CRF (left) and GRF (right) and analogues.

A hydrophobic spectral survey of the neuropeptides known to be present in the mammalian nervous system[71] (Table 3) led to the discovery of a unique secondary 8.0-residue mode in the 74-residue peptide ubiquitin. Fig. 15 shows the spectrum of a two-point moving average of the hydrophobic sequence which removed the omnipresent ~2.1-residue β-strand component (3.4 - 3.7 represents the α-helical segments).

Table 3
Hydrophobic Sequence Wavelengths

Peptide	Wavelengths		Peptide	Wavelengths	
	Primary	Secondary		Primary	Secondary
ACTH	2.35	13.3	Insulin A	4.00	3.08
Angiotensin II	4.00		Insulin B	5.33	
Atrial peptin I	4.00		β-LPH	4.44	
Atrial peptin II	4.44		LHRH	2.22	3.08
Bombesin	4.44	2.22	Motilin	2.86	
Bradykinin	2.22	3.08	α-MSH	2.17	
Calcitonin	3.64		β-MSH	2.67	
CCK-33	3.08		Neuropeptide Y	3.33	
CRF	2.11	4.44	Pancreatic polypeptide	3.33	2.00
β-Endorphin	4.44		Proctolin	2.50	
Gastrin	2.67		Secretin	4.44	3.33
GH	3.64		Somatostatin-28	13.3	4.00
GIP	5.00	2.67	Substance P	3.64	2.67
Glucagon	4.00	13.3	Ubiquitin	2.11	8.00
GRF	4.00		VIP	4.00	2.35

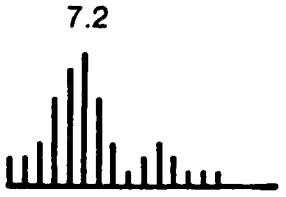

Fig. 15 Hydrophobic mode spectrum of ubiquitin.

A comparable 7 to 9-residue mode was found in the 53-residue epidermal growth factor (EGF)[72] as well as other peptides mitogenic for mesodermal and ectodermal tissues such as transforming growth factor (TGF) (Fig. 16).

Only a few receptors have been isolated and completely sequenced; among them is the EGF receptor protein.[73] The 126-residue extramembrane segment immediately following the 24-acid signal sequence was found to be dominated by a 7 to 9-residue mode that emerged again in the post-membrane, cytoplasmic domain. Extensive homology of the EGF and tyrosine kinase receptor related to oncogenesis suggests a potential role for the 7 to 9-residue mode in the regulation of oncogenes.[74]

Another recently sequenced receptor, for glucocorticoids,[75] was examined as a function of the average hydrophobicity of each ribosomal segment (~35 residues), and strong 7.5-residue peaks were found on both sides of the membrane, along with the common β, α, and ϵ (4.4 - 5) modes (Fig. 17). This suggested that some aspects of steroid actions might be mediated by a 7 to 9-residue hydrophobic mode, the implicit assumption being that the critical thermodynamic behavior of water mediates the mutual recognition of members of dissimilar chemical families, here the peptide receptor and non-peptide hormone.

We looked for evidence that the 7 to 9-residue mode that dominated ubiquitin, transforming growth factors and their receptor, and the glucocorticoid receptor, components of apparently quite diverse biological systems, had some meaningful common manifestation.

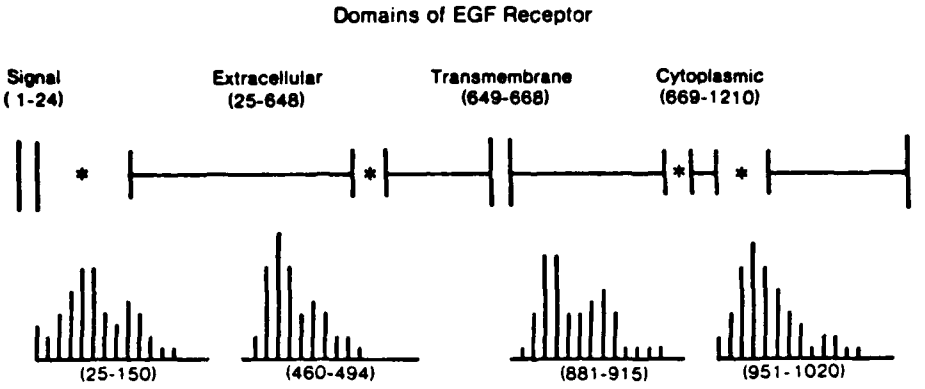

* Emergence of 7 to 9-residue wavelengths with 2-point moving average.

Wavelengths ~ 2.1 or 3.5 residues (β strands or α-helices) are present throughout.

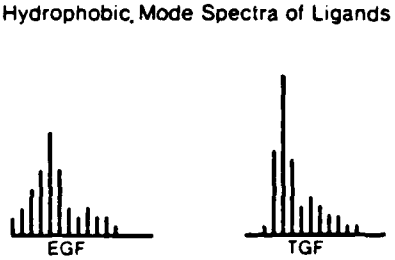

Fig. 16 Hydrophobic mode spectra of the EGF receptor and its peptide transmitters.

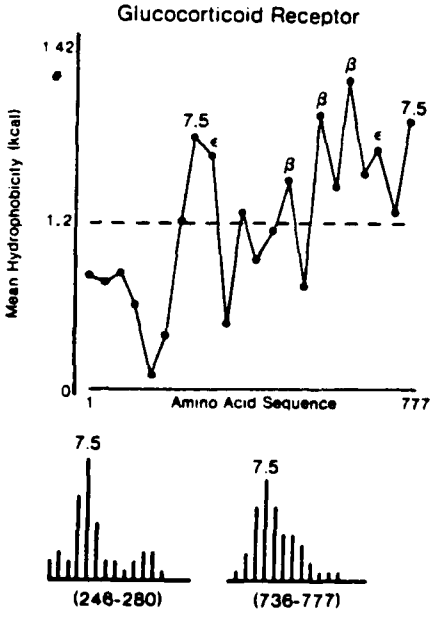

Fig. 17 Locations of the 7 to 9-residue hydrophobic modes as a function of segmental average hydrophobicity in the glucocorticoid receptor.

Resonant Mode-Induced Stimulation and Desensitization of a T_4-Lymphocyte Receptor by a Viral Complex Hydrophobic Mode

Ubiquitin, a peptide that becomes covalently conjugated to proteins marked for non-lysosomal proteolytic destruction,[76] has been found to be the reactive species in the lymphocyte cell outer membrane receptor.[77] Known to regulate the antigen-response competence of T- and B-cells via their maturation rates, ubiquitin, first isolated and sequenced from thymus by the Goldstein group (see [78] for review) also plays a prominent role in proteolytic systems active in the increased rate of degradation of abnormal proteins. A second functional aspect of the 7 to 9-residue hydrophobic mode of the ubiquitin-containing lymphocyte membrane receptor comes through its spectral ismorphism with the glucocorticoid receptor and the known cytotoxic and immunosuppressive actions of adrenal cortical hormones acting on T_4 lymphocyte subsets.[79] There are examples of "mode-resonant" desensitization of protein receptors on lymphocytes by high or prolonged levels of receptor peptide ligands associated with their internalization and degradation.[80,81]

The immunological failure, T_4-cell depletion,[82] and high incidence of neoplastic transformation in ectoderm and mesodermal tissues that characterize the acquired immunodeficiency syndromes (AIDS) suggested to us the possibility that the envelope sequences of the three responsible retroviruses might contain 7 to 9-residue hydrophobic modes as in the lymphocyte-ubiquitin-EGF-glucocorticoid receptor isometry. Recent reports of Addisonian signs of adrenal exhaustion and gland atrophy along with plasma ACTH elevation in patients with AIDS made us wonder if the viral peptide envelope might have activated and desensitized the receptors through a pseudo-corticoid mode resonance.[83–85] It is known that hydrocortisone greatly facilitates the isolation of retroviruses and their transmission to fresh leukocytes from AIDS patients.[86]

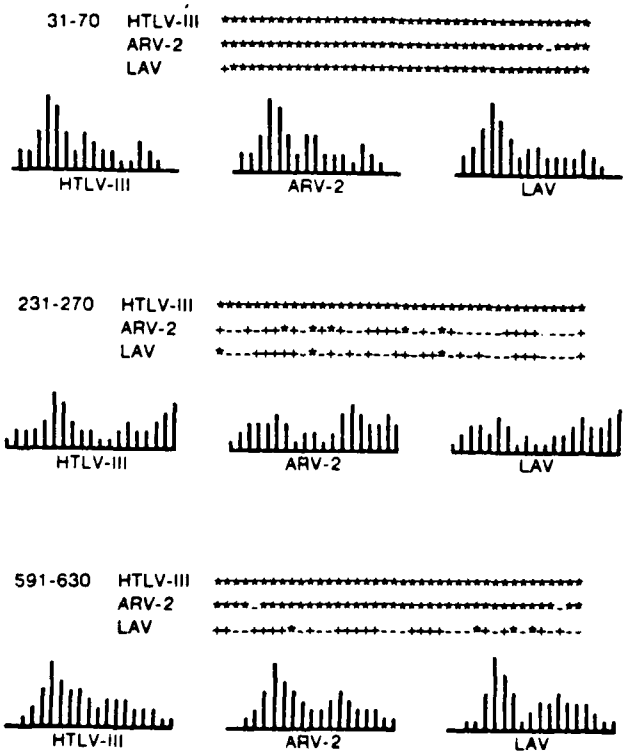

Fig. 18 The emergence of 7 to 9-residue hydrophobic mode wavelengths in the envelope proteins from three AIDS-related viruses. Amino acid hydrophobicities of HTLV-III were used as the reference (*); (+) and (-) show higher or lower kcal for corresponding residues on the other two viruses. In segment 31-70, which follows the putative signal sequence, ARV-2 and LAV are practically identical to HTLV-III, and similarity in hydrophobic mode spectra would be expected. However, similar spectra emerge in the extracellular domain between 231 and 270, where they differ from HTLV-III and from one another. A 7 to 9-residue wavelength appears between 591 and 630 where there is virtual identity between HTLV-III and ARV-2, which differ markedly from LAV. The prevalance of (+) and (-) precludes hydrophobically equivalent substitutions of amino acids as a basis for the spectral similarities and confirms the complexity of hydrophobic mode transformation.

Complex hydrophobic transformation showed 7 to 9-residue spectral modes in the envelope proteins of the AIDS-related viruses HTLV-III, ARV-2, and LAV[87–89] in the post-signal sequence segment and two other regions (Fig. 18). This led to a conjecture that the new anti-glucocorticoid steroids such as RU 486[90] might prevent, retard, or perhaps facilitate the hypothesized hydrophobic mode-resonant viral stimulation and desensitization of T-lymphocyte, EGF, and adrenal cortical membrane receptors by the AIDS viruses. The idea is currently being explored.

Appreciation is expressed to Mark Woyshville and Jim Cleveland for technical assistance; to Roger Guillemin, Fusun Zeytin, Mark Pollicott, and Michael Shlesinger for valuable discussions; to Dennis Sullivan for his stimulating lectures at the University of California, San Diego; and to the Protein Identification Resource of the National Biomedical Research Foundation, Georgetown University, Washington, D.C. This work is supported in part by DAAG20-83-K-0069 from the U.S. Army Research Office.

References

1. MANDELL, A. J., P.V. RUSSO & S. KNAPP. 1982. Strange stability in hierarchical coupled neuropsychobiological systems. *In* Evolution of Chaos and Order in Physics, Chemistry, and Biology. H. Haken, Ed. pp. 270-286. Springer-Verlag. Berlin.
2. MANDELL, A. J. 1986. Toward a neuropsychopharmacology of habituation: a vertical integration. Math. Modelling, in press.
3. MANDELL, A. J. 1984. Non-equilibrium behavior of some brain enzyme and receptor systems. Annu. Rev. Pharmacol. Toxicol. 24: 237-274.
4. MANDELL, A. J. & P. V. RUSSO. 1981. Striatal tyrosine hydroxylase activity: multiple conformational kinetic oscillators and product concentration frequencies. J. Neurosci. 1: 380-389.
5. RUSSO, P.V. & A. J. MANDELL. 1984. Metrics from nonlinear dynamics adapted for characterizing the behavior of non-equilibrium enzymatic rate functions. Anal. Biochem. 139: 91-99.
6. LEFFLER, J. & E. GRUNWALD. 1963. Rates and Equilibria of Organic Reactions. Wiley, New York.
7. LUMRY, R. & S. RAJENDER. 1970. Enthalpy-entropy compensation phenomena in water solutions of proteins and small molecules: a ubiquitous property of water. Biopolymers 9: 1125-1227.
8. TANFORD, C. 1973. The Hydrophobic Effect. Wiley-Interscience, New York.
9. JANIN, J. 1979. The protein kingdom: a survey of the three-dimensional structure and evolution of globular proteins. Bull. L'Inst. Pasteur 77: 337-373.
10. RUELLE, D. 1978. Thermodynamic Formalism. Addison-Wesley, Reading, MA.
11. MANDELL, A. J. 1978. Redundant mechanisms regulating brain tyrosine and tryptophan hydroxylases. Annu. Rev. Pharmacol. Toxicol. 18: 461-493.
12. GIBBS, J. W. 1873. A method of geometrical representation of the thermodynamic properties of substances by means of surfaces. Trans. Conn. Acad. II: 382-404.
13. KADANOFF, L. P. 1967. Static phenomena near critical points: theory and experiment. Rev. Mod. Phys. 39: 395-431.
14. BOWEN, R. 1974. Entropy versus homology for certain diffeomorphisms. Topology 13: 61-67.
15. HILBERT, D. 1971. Surfaces of constant gaussian curvature. *In* Foundations of Geometry. pp. 191-199. Open Court, La Salle, IL.
16. AHLFORS, L. V. 1979. Complex Analysis. McGraw-Hill, New York.
17. BLOCH, A. 1925. Les Théorèmes de M. Valiron, sur les fonctions entières et la théorie de l'uniformisation. Ann. Fac. Sci. Univ. Toul. 3: 17-26.
18. KUZMA, M. 1969. Fractional iteration of differentiable functions. Polon. Math. 22: 217-227.
19. RICE, R. E., B. SCHWEIZER & A. SKLAR. 1980. When is $f(f(z)) = az^2 + bc + c$? Am. Math. Month. 87: 252-263.
20. LI, T.Y. & J. A. YORKE. 1975. Period three implies chaos. Am. Math. Month. 82: 985-992.
21. SMALE, S. & R. F. WILLIAMS. 1976. The qualitative analysis of a difference equation of population growth. J. Math. Biol. 3: 1-4.
22. SULLIVAN, D. 1984. Quasiconformal homeomorphisms and dynamics II: structural stability implies hyperbolicity for Kleinian groups. IHES preprint.
23. AHLFORS, L.V. & S. SARIO. 1960. Riemann Surfaces. Princeton Univ. Press. Princeton.
24. SHENKER, S. J. 1982. Scaling behavior in a map of a circle onto itself: empirical results. Physica 5D: 405-411.
25. GREENE, J. M. 1979. A method for determining a stochastic transition. J. Math. Phys. 20: 1183-1201.

26. RAND, D., S. OSTLUND, J. SETHNA & E. D. SIGGIA. 1982. Universal transition from quasiperiodicity to chaos in dissipative systems. Phys. Rev. Lett. 49: 132-135.
27. KRUSHKAL, S. L. 1979. Quasiconformal mappings and Riemann Surfaces. Wiley. New York.
28. CURRY, J. H. & J. A. YORKE. 1978. A transition from Hopf bifurcation to chaos: computer experiments with maps on $\mathbf{R}^2$. Lect. Notes Math. 668: 48-66.
29. DENJOY, A. 1932. Sur les courbes définies par les equations differentielles à la surface du tore. J. Math. 17: 333-375.
30. HARDY, G.H. & E. M. WRIGHT. 1983. An Introduction to the Theory of Numbers. Oxford Univ. Press. Oxford.
31. MANDELBROT, B. B. 1980. Fractal aspects of the iteration of $z \to \lambda z(1 - \bar{z})$ for complex λ and z. Ann. N.Y. Acad. Sci. 357: 249-259.
32. WILLIAMS, R. F. 1955. A note on unstable homeomorphisms. Proc. Am. Math. Soc. 6: 308-309.
33. RUELLE, D. 1982. Repellers for real analytic maps. Ergod. Theor. Dynam. Sys. 2: 99-107.
34. CAYLEY, A. 1879. Application of the Newton-Fourier method to an imaginary root of an equation. Quart. J. Pure Appl. Math. 16: 179-185.
35. PEITGEN, H-O. & M. PRUFER. 1984. Global aspects of Newton's method for nonlinear boundary value problems. Forsch. Dyn. Syst. Univ. Bremen. Report # 114.
36. McDONALD, S. W., C. GREBOGI, E., OTT & J. A. YORKE. 1985. Fractal basin boundaries. Physica 17D: 125-153.
37. GREBOGI, C., E. OTT, S. PELIKAN & J. A. YORKE. 1984. Strange attractors that are not chaotic. Physica 13D: 261-268.
38. BLANCHARD, P. 1984. Complex analytic dynamics on the Riemann sphere. Bull. Am. Math. Soc. 11: 85-141.
39. HARDY, G. H. 1916. Weierstrass's non-differentiable function. Trans. Math. Soc. 17: 301-325.
40. SARKOVSKII, A. N. 1964. Co-existence of cycles of a continuous map of the line into itself. Ukrain. Mat. Z. 16: 61-71.
41. SALEM, R. 1943. Sets of uniqueness and sets of multiplicity. Trans. Am. Math. Soc. 54: 328-228.
42. SCHIKOF, W. H. 1984. Ultrametric Calculus, Cambridge Univ. Press, London.
43. SHLESINGER, M. F. & E. W. MONTROLL. 1983. On the wedding of certain dynamical processes in disordered materials to the theory of stable, Lévy, distribution functions. Lect. Notes Math 1035: 109-137.
44. HUBERMAN, B. A. & M. KERSZBERG. 1985. Ultradiffusion: the relaxation of hierarchical systems. J. Phys A Math. Gen. 18: L331-L336.
45. BLUMEN, A., J. KLAFTER & G. ZUMOFEN. 1986. Relaxation behavior in ultrametric spaces. J. Phys. A. 19: L77-L84.
46. SULLIVAN, D. 1982. Disjoint spheres, approximation by imaginary quadratic numbers, and the logarithm law for geodesics. Acta Math. 149: 215-237.
47. CARTWRIGHT, M.L. & J. E. LITTLEWOOD. 1945. On nonlinear differential equations of the second order. J. Lond. Math. Soc. 20: 180-189.
48. PASHLEY, R. M., P. M. McGUIGGAN & B. W. NINHAM. 1985. Attractive forces between uncharged hydrophobic surfaces: direct measurements in aqueous solution. Science 229: 1088-1089.
49. VAN DER POL, B. 1926. On relaxation oscillators. Phil. Mag. (Lond.) 2: 978-980.
50. COLE, K. S. 1972. Membranes, Ions, and Impulses. Univ. of California, Berkeley.
51. ARNOL'D, V. I. 1983. Geometrical Methods in the Theory of Ordinary Differential Equations. Springer-Verlag, Berlin.
52. TARGONSKY, G. 1981. Topics in Iteration Theory. Vandenhoeck, Göttingen.
53. POUNDER, J. R. & T. O. ROGERS. 1980. The geometry of chaos: dynamics of a nonlinear second-order difference equation. Bull. Math. Biol. 42: 551-597.
54. KADANOFF, L. P. & C. TANG. 1984. Escape from strange repellers. Proc. Natl. Acad. Sci. USA 81: 1276-1279.
55. BIRKHOFF, G. D. 1925. An extension of Poincaré's last geometric theorem. Acta Math. 47: 297-310.
56. CASDAGLI, M. 1986. Periodic orbits for dissipative twist maps. Doctoral Dissertation, University of Warwick.
57. BAMON, R., I. MALTA & M. J. PACIFICO. 1984. Changing rotation intervals of endomorphisms of the circle. PUC preprint, Brazil.
58. CHENCINER, A. 1983. Bifurcations de diffeomorphismes de $\mathbf{R}^1$ au voisinage d'un pointe fixe elliptique. *In* Chaotic Behavior of Deterministic Systems. G. Iooss, R. Helleman & R. Stora, Eds. pp. 273-348. North-Holland, Amsterdam.
59. DEVANEY, R. L. 1980. Linked twist mappings are almost Anosov. Lect. Notes Math. 819: 121-145.
60. ANOSOV, D. V. 1967. Geodesic flows on a compact Reimann manifold of negative curvature. Proc. Stek. Math. Inst. 90: 62-64.
61. MANNING, A. K. 1979. Topological entropy for geodesic flows. Ann. Math. 110: 567-573.

62. FENSTERMACHER, R. H., H. L. SWINNEY & J. P. GOLLUB. 1979. Dynamical instabilities and the transition to chaotic vortex flow. J. Fluid Mech. 94: 103-135.
63. MANDELL, A. J. 1986. Prime times: the distribution of singularities in hydrophobic free energy of proteins. *In* Perspectives in Nonlinear Dynamics. R. Cawley, A. W. Saenz, M. F. Shlesinger & W. Zachery, Eds. World Sci. Press. In press.
64. MANDELL, A. J. 1986. The hyperbolic nelix hypothesis: Stapleton's fractal measure on the hydrophobic free energy mode distributions of allosteric proteins. *In* Fractals in Physics. L. Pietronero & E. Tosatti, Eds. North-Holland, Amsterdam. In press.
65. STAPLETON, H. J., J. P. ALLEN, C. P. FLYNN, D. G. STINSON & S. R. KURTZ. 1980. Fractal form of proteins. Phys. Rev. Lett. 45: 1456-1459.
66. WAGNER, G. C., J. T. COLVIN, J. P. ALLEN & H. J. STAPLETON. 1985. Fractal models of protein structure, dynamics, and magnetic relaxation. J. Am. Chem. Soc. 107: 5589-5594.
67. NOZAKI, Y. & C. TANFORD. 1971. The solubility of amino acids and two glycine peptides in aqueous ethanol and dioxane solutions. J. Biol. Chem. 246: 2211-2217.
68. JIRGENSONS, B. 1973. Optical Activity of Proteins and Other Macromolecules. Springer, Berlin.
69. RIVIER, J., C. RIVIER & W. VALE. 1984. Synthetic competitive antagonists of corticoptropin releasing factor: effect on ACTH secretion in the rat. Science 224: 889-891.
70. GUILLEMIN, R., P. BRAZEAU, P. BOHLEN, F. ESCH, N. LING & W. B. WEHRENBERG. 1982. Growth hormone-releasing factor from a human pancreatic tumor that caused acromegaly. Science 218: 585-587.
71. IVERSEN, L. L. 1983. Nonopioid neuropeptides in mammalian CNS. Annu. Rev. Pharmacol. Toxicol. 23: 1-27.
72. COHEN, S. & G. CARPENTER. 1975. Human epidermal growth factor: isolation and chemical and biological properties. Proc. Natl. Acad. Sci. USA 72: 1317-1321.
73. ULLRICH, A., L. COUSSENS, J. S. HAYFLICK, et al. 1984. Human epidermal growth factor receptor cDNA sequence and aberrant expression of the amplified gene in A431 epidermoid carcinoma cells. Nature 309: 418-425.
74. COUSSENS, L., T. L. YANG-FENG, Y. C. LIAO, et al. 1985. Tyrosine kinase receptor with extensive homology to EGF receptor shares chromosomal location with neu oncogene. Science 230: 1132-1139.
75. HOLLENBERG, S. M., C. WEINBERGER, E. S. ONG, et al. 1986. Primary structure and expression of a functional human glucocorticoid receptor cDNA. Preprint.
76. CIECHANOVER, A., D. FINLEY & A. VARSHAVSKY. 1984. The ubiquitin-mediated proteolytic pathway and mechanisms of energy-dependent intracellular protein degradation. J. Cell. Biochem. 24: 27-53.
77. ST. JOHN, T., W. M. GALLATIN, M. SIEGELMAN, H. T. SMITH, V. A. FRIED & I. L. WEISSMAN. 1986. Expression cloning of a lymphocyte homing receptor cDNA: ubiquitin is the reactive species. Science 231: 845-850.
78. HERSHKO, A. & A. CIECHANOVER. 1982. Mechanisms of intracellular protein breakdown. Annu. Rev. Biochem. 51: 335-364.
79. PICHLER, W. J., A. EMMENDORFFER, H. H. PETER, et al. 1985. Analysis of T-cell subpopulations. Schweiz. Med. Wschr. 115+ 534-550.
80. KING, A. C. & P. CUATRECASAS. 1981. Peptide hormone-induced receptor mobility, aggregation and internalization. N.E.J.M. 305: 77-8o.
81. KOSMAKOS, F. C. & J. ROTH. 1980. Insulin-induced loss of the insulin receptor in IM-9 lymphocytes. J. Biol. Chem. 255: 9860-9869.
82. ZAGURY, D., J. BERNARD, R. LEONARD, et al., 1986. Long-term cultures of HTLV-III-infected T-cells. A model of cytopathology of T-cell depletion in AIDS. Science 231: 850-853.
83. TAPPER, M. L. 1984. Adrenal necrosis in the acquired immunodeficiency syndrome. Ann. Intern. Med. 100: 239-241.
84. GUENTHNER, E. E., S. L. RABINOME, A. VAN NIEL, A. NAFTILAN & R. G. DLUHY. 1984. Primary Addison's disease in a patient with the acquired immunodeficiency syndrome. Ann. Intern. Med. 100: 847-848.
85. GREENE, L. 1984. Adrenal insufficiency as a complication of the acquired immunodeficiency syndrome. Ann. Intern. Med. 101: 497-498.
86. MARKHAM, P. D. 1985. Advances in the isolation of HTLV-III from patients with AIDS and AIDS-related complex and donors at risk. Cancer Res. 45: 45885-45915.
87. RATHER, L., W. HASELTINE, R. PATARCA, et al., 1985. Complete nucleotide sequence of the AIDS virus, HTLV-III. Nature 313: 277-284.
88. SANCHEZ-RESCADOR, R., M. D. POWER, P. J. BARR, et al., 1985. Nucleotide sequence and expression of an AIDS-associated retrovirus (ARV-2). Science 227: 484-492.
89. WAIN-HOBSON, S., P. SONIGO, O. DANOS, et al., 1985. Nucleotide sequence of the AIDS virus, LAV. Cell 40: 9-17.
90. HEALY, D. L., G. P. CHROUSORS, H. M. SCHULTE, et al. 1983. Pituitary and adrenal responses to the anti-progesterone and anti-glucocorticoid steroid RU 486 in primates. J. Clin. Endocrinol. Metab. 57: 863-865.

END

2-87-

DTIC